Non-monotonic swelling of surface grafted hydrogels induced by pH and/or salt concentration

Gabriel S. Longo,[1,2,3] Monica Olvera de la Cruz,[3,4,5] and I. Szleifer[2,3,5,a]

[1]*Instituto de Investigaciones Fisicoquímicas Teóricas y Aplicadas (INIFTA), CONICET, La Plata, Argentina*
[2]*Department of Biomedical Engineering, Northwestern University, Evanston, Illinois 60208, USA*
[3]*Chemistry of Life Processes Institute, Northwestern University, Evanston, Illinois 60208, USA*
[4]*Department of Materials Science and Engineering, Northwestern University, Evanston, Illinois 60208, USA*
[5]*Department of Chemistry, Northwestern University, Evanston, Illinois 60208, USA*

We use a molecular theory to study the thermodynamics of a weak-polyacid hydrogel film that is chemically grafted to a solid surface. We investigate the response of the material to changes in the pH and salt concentration of the buffer solution. Our results show that the pH-triggered swelling of the hydrogel film has a non-monotonic dependence on the acidity of the bath solution. At most salt concentrations, the thickness of the hydrogel film presents a maximum when the pH of the solution is increased from acidic values. The quantitative details of such swelling behavior, which is not observed when the film is physically deposited on the surface, depend on the molecular architecture of the polymer network. This swelling-deswelling transition is the consequence of the complex interplay between the chemical free energy (acid-base equilibrium), the electrostatic repulsions between charged monomers, which are both modulated by the absorption of ions, and the ability of the polymer network to regulate charge and control its volume (molecular organization). In the absence of such competition, for example, for high salt concentrations, the film swells monotonically with increasing pH. A deswelling-swelling transition is similarly predicted as a function of the salt concentration at intermediate pH values. This reentrant behavior, which is due to the coupling between charge regulation and the two opposing effects triggered by salt concentration (screening electrostatic interactions and charging/discharging the acid groups), is similar to that found in end-grafted weak polyelectrolyte layers. Understanding how to control the response of the material to different stimuli, in terms of its molecular structure and local chemical composition, can help the targeted design of applications with extended functionality. We describe the response of the material to an applied pressure and an electric potential. We present profiles that outline the local chemical composition of the hydrogel, which can be useful information when designing applications that pursue or require the absorption of biomolecules or pH-sensitive molecules within different regions of the film. © 2014 AIP Publishing LLC. [http://dx.doi.org/10.1063/1.4896562]

I. INTRODUCTION

Stimuli-responsive hydrogels display large-reversible volume changes in response to specific modifications in their environment. In 1978, Tanaka[1] observed for the first time the collapse of polyacrylamide gels with either lowering the temperature or increasing the concentration of acetone in the buffer solution. These polymer hydrogels can be precisely designed to respond, with up to thousand-fold volume changes, to slight variations in an external perturbation of the medium, which can be chosen from a vast library of physical, chemical, and biological stimuli, including temperature,[1–3] solution pH,[4–6] and salt concentration,[5,7] applied electric field,[8,9] light exposure,[10] solvent composition,[4,11,12] and concentration of biomolecules.[13–16] Together, the magnitude of the externally controlled response, its reversibility, and the wide range of stimuli available make these hydrogels excellent candidates for a variety of applications requiring functional materials.

One of the most significant obstacles in developing hydrogel-based applications is the response-time, which is oftentimes prohibitively long.[17] Clearly, the use of hydrogels as the smart component of continuous biosensors,[18] muscle-like actuators,[19] microfluidic devices,[20] and many other applications require the volume transition to occur almost immediately following the stimulus. According to the theoretical predictions of Tanaka and Fillmore,[21] the stimulus-response time is approximately proportional to the square of the smallest spatial dimension of the hydrogel, which explains why large-sized hydrogels exhibit swelling that is significantly delayed with respect to the change in the environmental conditions. Therefore, the simplest way to achieve fast-responding hydrogels is to reduce one of its dimensions. Indeed, a response in the second timescale is expected for thin-hydrogel films having less than 10 μm in thickness.[21–23] Moreover, thin hydrogel films are more stable and easier to transport than grafted polymer layers.[22] Therefore, micro-/nano-sized hydrogel films are optimal candidates for the development of applications requiring fast and stable stimuli-responsive materials. Examples of their use include photonic[24] and tissue-adhesive[25]

a)Electronic mail: igal@northwestern.edu

materials, continuous glucose sensors,[18,26] and mechanical micro-actuators.[19,27] An excellent review of the applications of stimuli responsive thin films can be found in Ref. 22.

In the present study, we investigate the equilibrium response of a grafted hydrogel film composed of crosslinked polyacid chains when the pH and salt concentration of the bath solution are changed. The thickness of the film is in the scale of a few tens of nanometers and it varies depending on environmental (solution) conditions. In most experimental implementations, the hydrogel film is covalently bound to a solid surface. For this reason, swelling can only occur in the direction perpendicular to the plane of the substrate surface.[22,28] To study the properties of the grafted gel thin-film, we use a theoretical approach that explicitly accounts for the coupling that exists between molecular organization, chemical state of the monomers, and physical interactions. The approach is based on writing the system's free energy, including the conformational degrees of freedom of the network, the acid-base base equilibrium, ion confinement, and the electrostatic and van der Waals interactions.[29] Therefore, this approach can properly describe non-local charge regulation by the acid groups in the interior of the film due to the confined environment. At the same time, the theory allows for the incorporation of molecular information of the polymer network and other components, through the explicit account of the size, shape, and conformations of each molecular species in the system. In our previous study, we have predicted that when the film is physically deposited without interacting with the surface, the swelling process is not qualitatively different from a bulk hydrogel.[30] We now ask the question of how the constraint imposed by grafting some of the polymer chains to the substrate modifies the response of the material to the external stimuli. In this work, we show that interesting and non-trivial behavior arises from the interplay between all the aforementioned physicochemical contributions to the free energy, molecular organization, and spatial confinement.

The main findings from our earlier work in polyacid hydrogels[29,30] can be summarized as follows. The titration curves for the acid groups within the gel are much broader than those of the same group isolated in a bulk solution. Also, the so-called apparent pK_a, defined as the pH where half of the acid groups are protonated (deprotonated) is shifted to much higher values of pH. These two effects are the result of the interplay between the chemical free energy and the electrostatic interactions. Moreover, we have also predicted the dual role of the salt concentration to screen electrostatic interactions (lowering the relevance of electrostatic repulsions) while at the same time shifting the chemical equilibrium towards the deprotonated species, i.e., increasing the network charge. As a result, there is a non-trivial dependence of the gel swelling on the pH and salt concentration, and we have shown that the completely swollen gel does not necessarily correspond to a strongly charged network.

Finally, it is important to review what is known for grafted linear polyelectrolyte layers. In the case of a grafted layer of strong polyelectrolytes, the thickness of the film decreases monotonically when the concentration of monovalent salt is increased. Weak polyelectrolyte grafted layers present a richer behavior. For example in poor solvents, the addi-

tion of monovalent salt can help stabilize a layer that would otherwise collapse due to van der Waals attractions between polymer segments.[31] Moreover, increasing the salt concentration can lead to swelling of a grafted weak polyelectrolyte layer.[32] Theoretical calculations have predicted the thickness of grafted weak polyelectrolyte layers to have a maximum as a function of the salt concentration.[33,34] This behavior has been confirmed by experimental findings.[35] Is this non-monotonic behavior also present in grafted hydrogel films of weak polyacid chains? Are there important differences between grafted thin film gels and weak polyelectrolyte grafted layers? In this work, we report the reentrant swelling of thin film polyacid gels as a function of the ionic strength of the solution. Interestingly, a swelling-deswelling transition is also predicted at constant salt concentration when the pH of the solution is monotonically varied. In addition, we describe the response of the film to an applied pressure and an electric potential, and report the chemical composition of the system at different environmental conditions. This information can be useful in the targeted design of functional materials having a thin hydrogel film as the fast-acting smart component.

II. THEORETICAL APPROACH AND MOLECULAR MODEL

Consider a thin hydrogel film that is chemically grafted to a planar solid surface. The coordinate z measures the distance from the surface of total area A. This system is composed of a network of crosslinked polyacid chains and a solution that contains water (w), protons (H$^+$), hydroxyl ions (OH$^-$), and monovalent anions ($-$) and cations ($+$) due to dissociated added salt (NaCl, for example). Each unit of the network bears an acidic group that can be either protonated (AH) or deprotonated (A^-). Thus, the system of interest may be, for example, a thin film of polyacrylic acid gel. The film is in contact with a bulk solution of given pH and salt concentration, c. This solution provides a bath for all of the free species in the system and determines their chemical potentials. Our approach to study the thermodynamic behavior of this hydrogel film consists in defining a detailed molecular-level mean field theory. This molecular theory of weak polyelectrolyte gels, which is an extension of the molecular theory for grafted weak polyelectrolyte layers,[31,36] was first introduced to investigate swelling of a bulk hydrophilic polyacid gel in response to changes in the pH and salt concentration of the bath solution.[29] The initial step in this methodology consists in writing the total free energy of the system, which is given by

$$F = -T S_{\text{conf}} - T S_{\text{mix}} + U_{\text{vdw}} + U_{\text{st}} + F_{\text{chm}} + U_{\text{elec}}, \quad (1)$$

where T is the system temperature, S_{conf} is the conformational entropy of the flexible polymer network that makes the backbone of the hydrogel, S_{mix} is the translational entropy of the different free species in the solution, U_{vdw} is total attractive van der Waals interaction, U_{st} is the total repulsive steric (excluded volume) interaction, F_{chm} is the chemical free energy that accounts for the acid-base equilibrium of the titratable segments of the polymer network, and U_{elec} is the total electrostatic energy. Each of these terms of the free energy can

be explicitly expressed as a functional of the probability of the different molecular conformations of the network, the local density profiles of the mobile species, the local degree of charge of the network, and the position-dependent electrostatic potential. Finding the extremum of F with respect to the aforementioned functions leads to a series of equations that are numerically solved to calculate the local interaction fields (the osmotic pressure and the electrostatic potential). All structural properties of the system can be then obtained from the probabilities of the different network conformations, and the interaction fields. Furthermore, any relevant thermodynamic quantity can be directly derived from the free energy of the system, which is known at this point. A more thorough description of the methodology can be found in Refs. 29 and 30, as well as in the supplementary material.[37]

This theory is general and can therefore be applied to the study of any polyacid hydrogel film, regardless of the architecture of the polymer network. The molecular details of the polymeric structure enter the theoretical framework through the set configurations via the local density distribution, which is an input of the theory. We have already applied the present approach to investigate the isotropic swelling in response to stimuli of a pH-sensitive film physically deposited on a planar surface.[30] In this work, we study the behavior of a thin hydrogel film having some of the weak polyacid chains chemically grafted to the surface, such that the film can only swell in the direction perpendicular to the surface when the stimulus is applied. The molecular model of the grafted film considered is illustrated in Fig. 1. Each chain in the network has 25 monomers. Most of the polymer chains connect two crosslinks, except topmost chains that have their solution-side ends free, and the chains that are grafted by one of their ends to fixed positions on the planar surface. The functionality of each crosslink is six. Grafting points are arranged in a square lattice with area density σ. In the completely elongated conformation of the network, the free chains are located exactly on top of the grafting points (i.e., same x and y). For each grafting density, a large set ($\sim 10^4$) of independent conformations is generated using 10 ns long Molecular Dynamics (MD)

simulations at room temperature, and recording one configuration every picosecond. We assume that the polymer backbone is hydrophilic. The logarithmic acidity constant is taken as $pK_a = 5$ to represent a carboxylic acid such as acrylic acid.[38] More details on the molecular model of the grafted hydrogel film and the MD simulations performed to obtain the set of conformations can be found in the supplementary material.[37]

III. RESULTS

A. Film local organization

We begin by discussing the local variation of the pH as well as the difference in the pH within the film as compared to the bulk solution. Before we show results, it is important to emphasize how we define the local pH. The thermodynamic definition is given by $pH = -\log_{10} a_{H^+}$, where a_{H^+} is the activity of the protons. Thermodynamic equilibrium requires equal chemical potential everywhere which implies equal pH, since the chemical potential is given by a constant plus the logarithm of the activity. In general, however, one refers to the pH in terms of the molar concentration of protons. Thus, we define the local pH, as $pH(z) = -\log_{10}[H^+](z)$, where $[H^+](z)$ is the local molar concentration of protons. This quantity is important because it is related to the local degree of protonation. Figure 2(a) shows typical examples of local pH curves as a function of the distance from the grafting surface. Each profile consists of three distinctive regions. Sufficiently far from the surface, the local pH approaches that of the bath solution. Inside the gel, close to the surface, a lower pH is established. We define the gel pH as the average of the local pH over the extension of the film,

$$pH_{gel} = \frac{1}{h}\int_0^h pH(z)dz, \qquad (2)$$

where h is the film thickness. The gel pH is shown as a dotted line for each of the profiles shown in Fig. 2(a). Except for the relatively small variation due to the structure of the
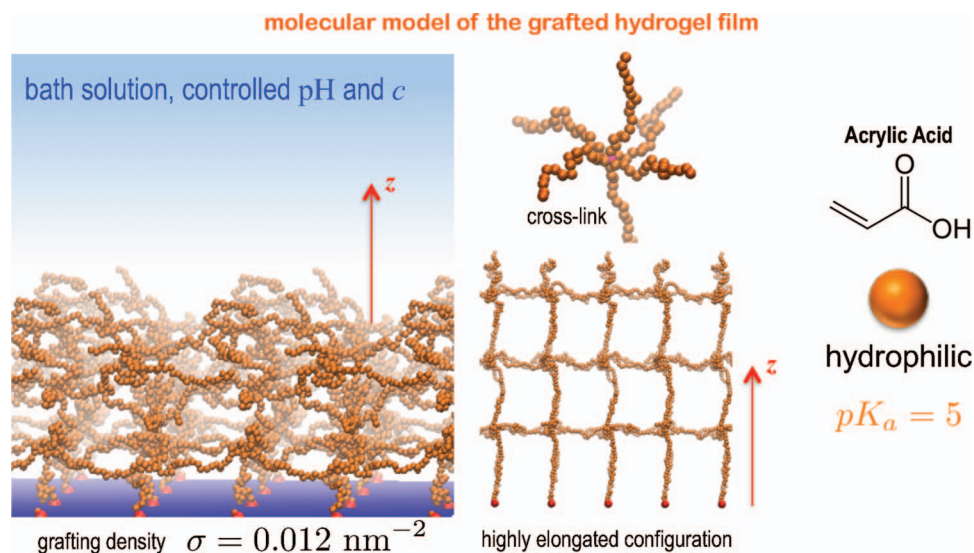

molecular model of the grafted hydrogel film

bath solution, controlled pH and c

cross-link

Acrylic Acid

hydrophilic

$pK_a = 5$

grafting density $\sigma = 0.012 \text{ nm}^{-2}$ highly elongated configuration

FIG. 1. Schematic representation of the chemically grafted polyacid hydrogel film. The surface sits at $z = 0$.

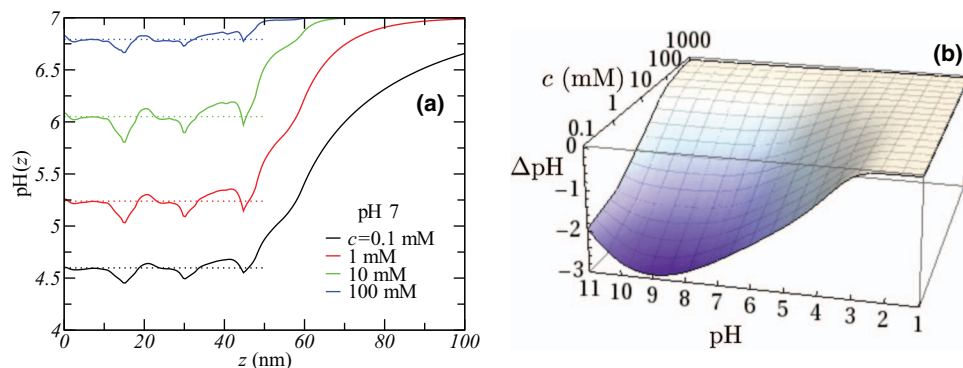FIG. 2. (a) Local pH *vs.* distance from the surface at pH 7 and different c. Dotted lines correspond to pH_{gel}. (b) $\Delta pH = pH_{gel} - pH$ as a function of both pH and c. In both panels, the grafting density is $\sigma = 0.012$ nm^{-2}.

network (the lower pH spikes can be associated to the most-likely z-coordinate of the crosslinks, which have consequently the highest polymer density), pH_{gel} gives accurate quantitative information of the acidity in the interior of the hydrogel film. Panel (b) of the figure shows the drop in pH in the interior of the gel, $\Delta pH = pH_{gel} - pH$, for all the pH and c range considered in this work. ΔpH depends critically on the composition of the bath solution. For the thin film that we have considered, which spans less than 100 nm in height, the magnitude of the drop in pH can reach as much as three units under certain conditions. As we discuss in detail below, when we describe the degree of protonation of the network, the changes in pH are due to a local Le Chatelier shift in the chemical equilibrium in order to reduce the local electrostatic repulsions.

The last region remaining to describe is the one that contains the interface between the film and the bulk solution. Within this transition zone the local pH varies from its bath value to pH_{gel}. The width of this region, which can extend longer than the gel itself at low c, depends mainly on the salt concentration, because it is effectively determined by the Debye length on the bulk solution. The Debye length of a solution gives a measure of the effective extent of the electrostatic interactions. The position-dependent density profiles of other free ions at different compositions of the bath solution are presented in the supplementary material.[37]

B. Reentrant swelling: The role of pH and salt concentration

Because the polymer network is chemically grafted, the gel can only swell in the direction perpendicular to the plane

of the supporting surface. Therefore, the state of swelling is fully characterized by the height or thickness of the film,

$$h = \frac{\int_0^\infty 2z \langle \rho_p(z) \rangle dz}{\int_0^\infty \langle \rho_p(z) \rangle dz}, \tag{3}$$

defined as twice the first moment of the normalized z-dependent density of monomers. In Eq. (3), $\langle \rho_p(z) \rangle$ is the ensemble average local density of polymer at z. Figure 3 shows the height of the hydrogel as a function of the salt concentration and the pH of the bath solution. The distance between grafting points ($\sigma^{-\frac{1}{2}}$) is different for each of the three hydrogels displayed in the figure. Note that the average volume fraction of polymer, ϕ_p, is proportional to σ, and it increases with increasing grafting density. However, since ϕ_p is also inversely proportional to h, it varies with the composition of the bath solution. For this reason, we use σ instead of ϕ_p to characterize the film. The predictions shown in Fig. 3 reveal a very interesting swelling behavior of grafted hydrogels. A reentrant behavior, having both a region where the film swells (h increases) and another where it deswells (h decreases), is predicted when either the pH or c are increased monotonically. The figure illustrates that although the swelling behavior is qualitatively similar for all of the grafting densities presented, the quantitative details of the transition depend on the molecular architecture of the gel.

To better understand the swelling behavior of the film, Figure 4(a) shows its thickness as function of the bath pH at various salt concentrations and a given grafting density, together with the average degree of protonation shown in Figure 4(b). At low pH, h takes the smallest value, which is independent of c, while at high pH the hydrogel is in a swollen
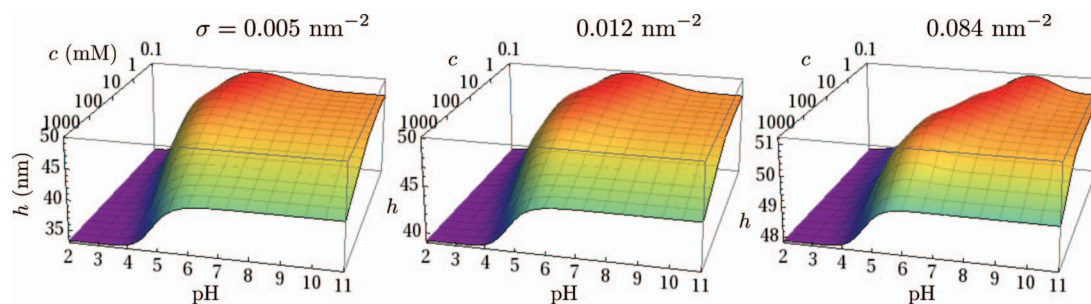

FIG. 3. Film thickness, h, *vs.* pH and c at different grafting densities.
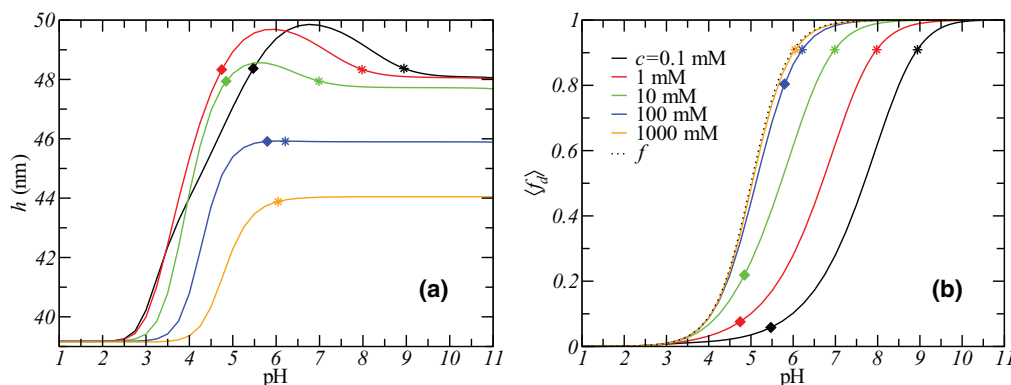
FIG. 4. Film height (a) and average degree of dissociation (b) as a function of the solution pH, at different ionic strengths and $\sigma = 0.012$ nm^{-2}. The stars correspond to the pH at which $\langle f_d \rangle = \frac{10}{11}$, indicating that approximately 90% of the monomers are dissociated. Each diamond gives the point along the curve having the same ordinate (film height) as the corresponding star. f gives the degree of dissociation of an isolated acid group in a dilute solution.

state whose thickness depends strongly on the ionic strength of the solution. The swelling transition as a function of pH is not monotonic, except for the case of very high salt concentration considered. The highest extension of the film corresponds to a local maximum of the curve that occurs at an intermediate pH. In the next paragraph, we outline the conditions that enable us to understand the origin of this reentrant swelling-deswelling transition.

The fraction of deprotonated isolated monomers in a dilute (or ideal) solution is given by the well-known expression

$$f \equiv f(\text{pH}) = \frac{1}{1 + 10^{(\text{pK}_a - \text{pH})}}. \quad (4)$$

Given the intrinsic pK$_a$ of the acid, f is a monotonically increasing single-variable function of the solution pH. In such a system, the transition from the uncharged to the charged species occurs within two units of pH around pK$_a$. Less than 10% of the molecules are dissociated at pH $=$ pK$_a - 1$, while more than 90% of the groups are charged at pH $=$ pK$_a + 1$. More precisely, $f(\text{pK}_a - 1) = \frac{1}{11}$ and $f(\text{pK}_a + 1) = \frac{10}{11}$. The position average degree of dissociation of network monomers, in the hydrogel film, can be calculated using

$$\langle f_d \rangle = \frac{\int_0^\infty f_d(z) \langle \rho_p(z) \rangle dz}{\int_0^\infty \langle \rho_p(z) \rangle dz}, \quad (5)$$

where $f_d(z)$ is the local degree of dissociation of the network, and the product $f_d(z) \langle \rho_p(z) \rangle$ gives the local charge density of the network.

To understand the titration curves shown in Fig. 4(b), we need to consider the role of confinement on the chemical equilibrium of the acid groups of the network. Large degrees of dissociation lead to high confinement of charges and large electrostatic repulsions. Lowering the degree of deprotonation reduces the electrostatic repulsions at the cost of chemical free energy. The transition in $\langle f_d \rangle$ occurs at higher pH values than that of the ideal solution, as can be observed in panel (b) of Fig. 4, demonstrating that the system prefers to pay in chemical free energy in order to avoid large electrostatic repulsions. There are two additional components that need to be considered. One is the swelling of the gel that increases the effective distance between charged monomers, and thus it reduces

the electrostatic repulsions. Second, there is the adsorption of salt ions that screens the electrostatic repulsions, thus reducing both the chemical free energy and the electrostatic repulsions penalty. However, the adsorption of ions results in a large entropic price associated with counter ion confinement. This free energy cost increases as the salt concentration in the bulk decreases. The balance between all these four components leads to the titration curves predicted in Fig. 4(b). As the salt concentration decreases, there is a larger shift of the degree of dissociation curve towards higher values of pH. Then, the electrostatic repulsions and the counter ion confinement dominate, and the system pays in chemical free energy, resulting in a larger shift of $\langle f_d \rangle$ from the ideal solution value. When the salt concentration increases the screening is more prevalent, and consequently the gel can be charged at lower pH values. Thus, we see the dual role of salt of screening the electrostatic interactions and charging the gel. These two effects go in opposite directions in determining the swelling of the network. As a manifestation of this dual role of the salt, we observe the reentrant swelling of the film. Note that for relatively high salt concentration this effect disappears, the titration curves look very similar to the ideal solution behavior, and the film thickness is monotonic in pH.

We quantify the condition of a charged network with the criteria $\langle f_d \rangle = \frac{10}{11}$. The film thickness at the pH where this equality is fulfilled is marked by a star in panel (a) of Fig. 4. The swelling transition is mostly complete at this point, and the gel height has reached a plateau region. In other words, once the network is highly charged increasing the pH does not lead to further swelling. However, the highly charged network does not correspond to the maximum swelling of the hydrogel. If we draw a horizontal line (parallel to the pH axis) that intersects the h vs. pH curve at the star, this line also cuts across the curve at a lower pH, marked in Fig. 4 using a diamond. These two values of pH delimit the region of non-monotonic swelling (swelling-deswelling). The degree of dissociation at the state given by the diamond depends strongly on the salt concentration as can be seen in Fig. 4(b). At the low pH branch of the region of non-monotonic behavior, the film is weakly charged at low c, but strongly charged at high c.

The characteristics of the non-monotonic behavior can be observed more clearly by looking at different properties
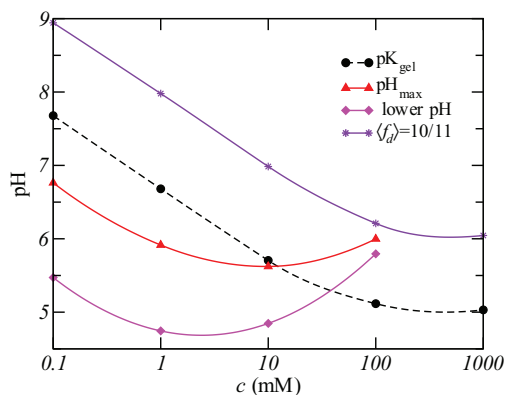
FIG. 5. The figure illustrates the dependence on the salt concentration of the key points that characterize the region of non-monotonic swelling. The pH values that correspond to the lower (magenta curve, diamonds) and upper (purple curve, stars) bounds of this region are shown, which coincide with the diamonds and stars of Fig. 4, respectively. The range of pH where swelling-deswelling behavior is predicted is bounded by the magenta and purple curves. The figure also shows the pH at which the film achieves maximal thickness, pH_{max}, which is obviously contained within such region. In addition, the apparent pK_a of the network, pK_{gel}, is presented as a function of c.

FIG. 6. Concentration of positively charged ions inside the gel, $[i_+]$, vs. pH, at different salt concentrations, c. The grafting density is $\sigma = 0.012$ nm^{-2}. Diamonds and stars correspond to the same conditions of Fig. 4.

of the hydrogel that characterize the acid-base equilibrium in relation to the swelling. Figure 5 shows the apparent pK_a of the gel monomers, pK_{gel}, as a function of the salt concentration. This quantity is defined as the pH at which the fraction of protonated monomers is exactly one half ($\langle f_d \rangle = \frac{1}{2}$). Additionally, Fig. 5 shows the dependence on c of the two values of pH that delimit the region of reentrant swelling-deswelling behavior (i.e., those that correspond to the diamonds and stars of Fig. 4). The intermediate pH at which maximum swelling is achieved, pH_{max}, is also displayed in the figure as a function of the salt concentration. pK_{gel} marks the midpoint in the transition from a low to a highly charged network. This quantity is always above the intrinsic pK_a of the monomer ($pK_a = 5$) due to the interplay between chemical free energy and electrostatic repulsions, as discussed above. The lower-pH limit of the swelling-deswelling transition (diamonds joint by the magenta curve in Fig. 5) can occur at either side of pK_{gel}, meaning that the network can be either weakly or strongly charged at the onset of the non-monotonic behavior. The same is true for the pH at which the maximal thickness is predicted (triangles joined by the red curve in Fig. 5). These results imply that the maximum swelling may correspond to either a weakly or highly charged network. Another observation from Figs. 4 and 5 is that the width of the region of non-monotonic behavior, defined as the pH of the star minus that of the diamond, decreases monotonically with c (see the supplementary material[37]) until it vanishes as the salt concentration approaches 1 M.

One of the most interesting manifestation of the grafting of the thin film gel is the dependence of the width of the swelling transition on the salt concentration. Looking at Figs. 4 and 5 we see that the width of the transition (from collapsed at low pH to either the maximum swelling or the final plateau at high pH) increases with decreasing salt concentration. The width of the titration curve also increases with decreasing salt concentration. In the case of a bulk polyacid
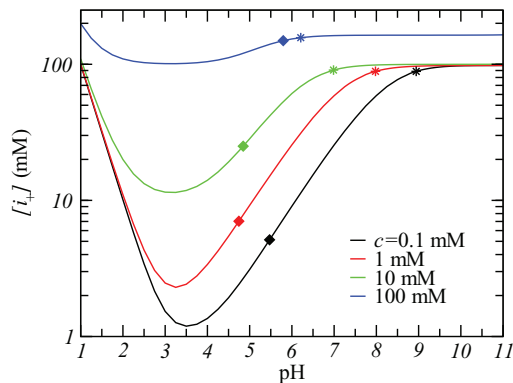
gel[29] and a physically deposited polyacid film,[30] the width of the titration curve also increases with decreasing salt concentration. However, the behavior of the width of the swelling transition shows exactly the opposite behavior. Namely, the width decreases with decreasing salt concentration. Therefore, we see two main features that show qualitative different behavior in grafted gels, as presented here, from the behavior predicted in bulk and surface supported gels. The presence of a local maximum on the swelling and the increase of the width of the transition with decreasing salt concentration. These two effects are manifestations of the chemical grafting of some chains of the gel onto the surface that only allow for swelling in one direction.

In order to elucidate the origin of the reentrant behavior observed in the pH-dependent swelling, Figure 6 shows the concentration of counter ions inside the hydrogel as a function of pH, at the same conditions of Fig. 4. The quantity $[i_+]$ gives the average concentration of positively charged mobile molecules inside the film (i.e., from $z = 0$ to $z = h$). Within the region of non-monotonic swelling, denoted between the stars and the diamonds, the concentration of counter ions increases with pH. The non-monotonic response of the film can be explained by the competing effects that an increasing ionic concentration has in modulating the interplay between the acid-base equilibrium and the intra-network electrostatic repulsions. Interestingly, the concentration of free ions within the film when $\langle f_d \rangle = \frac{10}{11}$ is of the order of 100 mM and therefore, it is completely controlled by the charge in the polymer. In order to compete with this large concentration of confined counterions, the chemical equilibrium is shifted one unit of pH each by going from $c = 0.1$ mM to $c = 1$ mM to $c = 10$ mM. For the low end of deprotonation, we see that the concentration of ions within the film depends on the solution salt concentration. The salt concentration between the two limits explains also why for $c = 100$ mM the presence of the non-monotonic behavior disappears.

The non-monotonic behavior predicted as a function of the solution ionic strength at fixed pH, see Fig. 3, has been similarly predicted for grafted polymer layers of weak polyelectrolytes. In the latter case, scaling considerations, self-consistent field theory, and molecular theory[32–34,39] have all
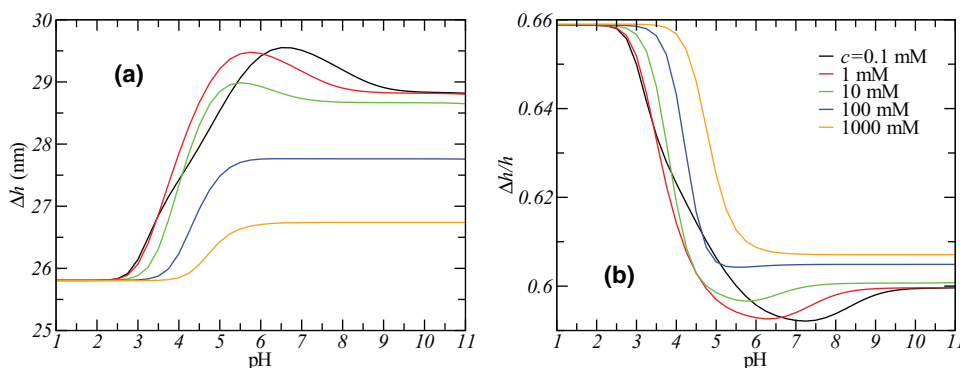
FIG. 7. Absolute (a) and relative (b) fluctuations in the film height as a function of the solution pH, at different ionic strengths and $\sigma = 0.012$ nm^{-2}.

provided the same qualitative picture. The maximum has been experimentally observed.[35] Similarly, the radius of star-branched weak polyelectrolytes was calculated to have a maximum as a function of the ionic strength by a self-consistent-field model.[40] Recently, a reentrant swelling-to-collapse transition was theoretically predicted for micrometer-sized (or larger) weak polyelectrolyte gels in good solvent, assuming local electroneutrality.[41] The authors explain that initially, increasing c promotes dissociation until $\langle f_d \rangle$ saturates once it reaches the value of the dilute solution. Adding more salt to the solution can only reinforce the screening of the electrostatic repulsions, and thus the gel begins to deswell. We also attribute the non-monotonic swelling behavior of the grafted hydrogel film to the opposing effects that increasing c promotes. In our study, however, we do not observe a clear correlation between the saturation of the degree of charge of the polymer network and the resulting reentrant behavior. Namely, our predictions suggest that the reentrant swelling is the result of the delicate balance between chemical free energy, electrostatic repulsions, the molecular organization of the gel, and the dual role of salt in screening and charging.

C. Prediction of experimental observables

The (absolute) fluctuations in the thickness of the hydrogel film are given by

$$\Delta h = \sqrt{\langle h^2 \rangle - h^2}, \qquad (6)$$

where $\langle h^2 \rangle$ is defined, analogously to h, as proportional to the second moment of the normalized density distribution of monomers, which is

$$\langle h^2 \rangle = \frac{\int_0^\infty (2z)^2 \langle \rho_p(z) \rangle dz}{\int_0^\infty \langle \rho_p(z) \rangle dz}. \qquad (7)$$

The fluctuations in h are shown in Fig. 7 (panel (a)) as a function of the pH, together with the relative fluctuations (panel (b)), $\frac{\Delta h}{h}$. A visual comparison between Figs. 4(a) and 7(a) shows the similar dependence of h and its absolute fluctuations on both pH and c. Relative to the film thickness, however, these fluctuations decrease as the gel swells, and they have a global/local minimum near the pH of maximum swelling. This behavior is likely the consequence of the loss of conformational degrees of freedom of the polymer network

as the chains are stretched when the volume of the film increases. The relative fluctuations in height are very large. At maximum swelling the film extends, at most, 2 nm more than in the high-pH region. The fluctuations in thickness, however, are an order of magnitude larger than that difference. The reason for such large fluctuations in h may be related to the molecular architecture of the network. By definition, h is proportional to the first moment of the distribution of mass of the monomers. Due to the molecular structure of the network, the polymer chains are more likely to occupy the region exactly above the grafting points, which can lead to heterogeneous height in the $x - y$ plane. These large fluctuations might prevent experimental observation of the pH-dependent non-monotonic swelling of nano-sized grafted polyacid hydrogel films. However, a reentrant swelling of comparable magnitude has been experimentally observed as a function of the salt concentration in grafted weak polyelectrolyte layers of similar thickness.[35]

Next, we ask if the height fluctuations modify the response of the material to an external stimulus. This question can be addressed by investigating the isothermal compressibility of the polymer network, κ_T, which measures the relative volume change of the polymer network in response to an applied mechanical force. This quantity is related to the fluctuations in thickness through the following expression (see the supplementary material[37]):

$$\kappa_T = -\frac{1}{V} \left(\frac{\partial V}{\partial P} \right)_T = -\frac{1}{h} \left(\frac{\partial h}{\partial P} \right)_T$$
$$= \frac{A(\Delta h)^2}{k_B T h}, \qquad (8)$$

where $V = Ah$ is the volume of the film, and P is the applied pressure. κ_T shows a non-monotonic dependence on both the pH and the ionic strength of the bath solution, as can be observed in Fig. 8. The response of the material to compression can be qualitatively explained by considering its two main contributions. On the one hand, compression is favored (κ_T raises) by the increase of the conformational entropy of the network, when the hydrogel is in a swollen state and the polymer chains are elongated beyond their equilibrium length. As the gel is compressed, on the other hand, solvent is expelled from the interior film. The expulsion of ions, in particular, disfavors compression because it reduces the screening of the
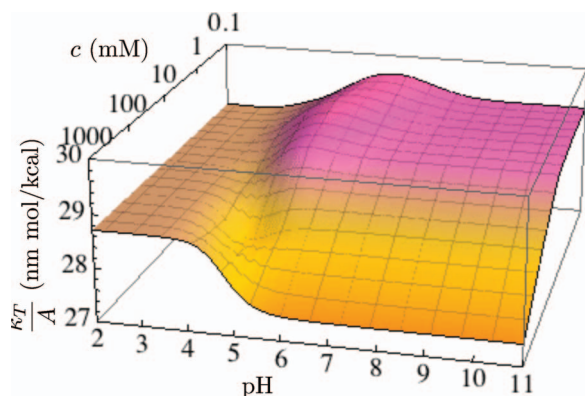
FIG. 8. The isothermal compressibility of the polymer network per unit area as function of the bath pH and salt concentration, $\sigma = 0.012$ nm^{-2}, and $T = 25\,^\circ$C.

FIG. 9. The capacitance of the hydrogel film as a function of the pH at different salt concentrations.

electrostatic repulsions between charged monomers. At low c, the film can be compressed without a considerable expulsion of the relatively few confined ions, so the main contribution to the response of the material is the change in the conformational entropy of the network. Therefore, κ_T shows a non-monotonic dependence on the pH that correlates directly with that of h under the same conditions (shown in Fig. 4). In other words, as the hydrogel swells its compressibility increases. However, as c increases, and a growing number of ions are adsorbed inside the hydrogel, compression of the film leads to a significant expulsion of ions. When the concentration of salt is high enough, the strengthening of the electrostatic repulsions between monomers is the dominant factor in determining κ_T, which shows an inverse correlation with the film thickness as pH increases. Interestingly, the results presented in Fig. 8 indicate that there is a salt concentration in between 10 and 100 mM for which the response of the material to an applied pressure is barely sensitive to pH. It is compelling that this range of salt concentrations is close to that of physiological relevance, i.e., around 100 mM, suggesting a buffering effect that may stabilize the response of systems to concentration fluctuations.

Another quantity that can be used to describe the response of the film is its capacitance, C_f, which quantifies the ability of the hydrogel to store electric charge (or energy) when placed on the metallic surface of an electrode. The capacitance of a material measures the differential change in the area density of electric charge on the surface of the metal, σ_M, with respect to an infinitely small change in the applied electrostatic potential, ΔV; that is,

$$C_f = \left(\frac{\partial \sigma_M}{\partial \Delta V} \right). \tag{9}$$

Polymer hydrogels with a high capacitance per unit volume are of interest in the development of supercapacitors.[42,43] This quantity is well known to depend on the composition of ionic or ionizable molecular species in the region near the electrode.[44–47] In other words, the capacitance depends on the ability of the environment that surrounds the electrode to screen the electric charge on the surface of the metal. The capacitance of the film as function of pH is shown in Fig. 9 at different salt concentrations. In order to account for
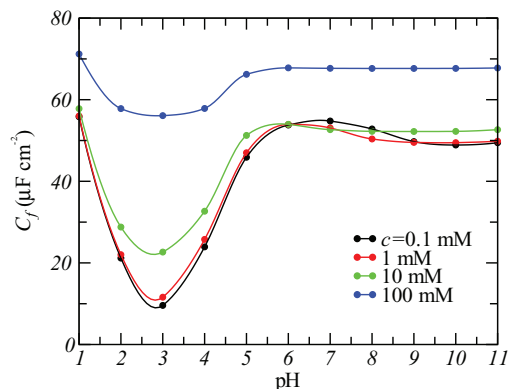
the metallic surface when calculating C_f, the boundary conditions of the Poisson equation are modified from constant surface charge density to constant electrostatic potential on the surface. The surface charge density shows a linear dependence on the applied potential within all the range of voltages considered in this work, from -10 to 10 mV (see the supplementary material[37]). We observe that the film capacitance is highly correlated with the adsorption of counter ions, shown in Fig. 6, due to the screening of the electrode charge. Notice, however, that *a priori* the concentration of ions inside the film depends on the applied voltage, while no electrostatic potential was applied to obtain the results presented in Fig. 6.

IV. DISCUSSION AND CONCLUSION

We have applied a molecular theory to study the thermodynamics of a grafted weak polyacid hydrogel, with particular attention in the response of the material to changes in the pH and salt concentration of the bath solution that is in equilibrium with the film. The novel prediction of this work is the pH-dependent non-monotonic swelling of the film. This non-monotonic behavior occurs only if the film is chemically grafted to the surface. This implies that the behavior of chemical grafted thin film gels is different from those that are just supported on the surface[30] or from bulk weak polyelectrolyte gels.[29] The difference is due to the constrain of only being capable of swelling in the direction perpendicular to the grafting surface.

At most salt concentrations, the grafted gel first swells as the pH increases, until its thickness finds a local maximum. A subsequent raise in the pH causes the film to deswell until its height reaches a plateau region where increasing the pH further does not modify the volume of the system. This behavior results mainly from competition between charge regulation by the polymer titratable groups (acid-base equilibrium) and the electrostatic repulsions between charged monomers, which are both modulated by the absorption of ions and the ability of the network to modify its volume. However, due to the complex coupling existing between those contributions to the free energy, it is not possible to describe the onset of the pH-dependent reentrant behavior in terms of a single computable variable, for example, the average degree of dissociation or

the concentration of absorbed counter ions. At very high salt concentrations in solution, the competition disappears due to the very high screening of the electrostatic interactions, and we predict monotonic swelling as the pH increases. For example, the width of the region where swelling-deswelling is observed decreases as the salt concentration of the solution increases. In addition, if the conditions are such that $\langle f_d \rangle$ is close to the degree of charge of the acid group measured in a dilute solution (e.g., for the film in contact with a highly saline solution), the chemical free energy is near its optimal value, and the thickness of the film is a monotonically non-decreasing function of the pH.

In this work, we define the height of the film as proportional to the first moment of the polymer density distribution,[33,39] see Eq. (3). There is, however, an alternative definition, termed the total thickness in what follows, that can be obtained using the distance from the surface at which the polymer density profile vanishes.[32] That is, h_{tot} such that $z \geq h_{tot}$ implies $\langle \rho_p(z) \rangle = 0$. Lyatskaya et al.[32] showed that the two definitions of thickness are generally not equivalent for weak polyelectrolyte layers. While the first moment of the density distribution possesses a maximum as a function of the salt concentration, the total thickness presents a monotonic dependence on c. We argue that h is a more representative quantity of the response of the material, in particular, to an applied external force. In a molecular-level description of the hydrogel film, the total thickness can be rather insensitive to changes in the chemical composition of the solution, because the definition of h_{tot} requires, for example, that the probability of all network conformations having one or more monomers above that height to be exactly zero. The relative fluctuations in film thickness are calculated to be very large, which might hinder experimental observation of the non-monotonic swelling transition. These fluctuations may reflect the molecular architecture and highlight the heterogeneity of the polymer network. Full three-dimensional calculations are being carried out to evaluate such speculation.

We further predict that the film height can also present a non-monotonic dependence on the salinity of the solution, at fixed pH. This reentrant behavior is due to the coupling between charge regulation and the two opposing effects triggered by the addition of salt to a weak polyelectrolyte system. At higher or lower pH values, the grafted hydrogel film deswells monotonically if the ionic strength of the solution increases. Weak polyelectrolyte systems are known to exhibit such reentrant behavior in presence of a monovalent salt as a consequence of charge regulation. Adding monovalent salt to the system can help stabilize grafted weak polyelectrolyte layers, instead of inducing the collapse of the polymer chains, as a function of grafting density and solvent quality.[31] Moreover, the thickness of weak polyelectrolyte layers has been predicted to be a non-monotonic function of salt concentration by theoretical considerations.[32–34,39] Further, this effect has been observed experimentally for polyacrylic acid grafted polymers,[35] and was quantitatively predicted using the molecular theory.[34] Interestingly, the magnitude of the observed thickness and non-monotonicity are similar to those calculated here for the thin film gel. Swelling-deswelling behavior has been theoretically predicted for star-

branched weak polyelectrolytes[40] and weak polyelectrolyte microgels.[41] Reentrant behavior in terms of the solvent composition has been reported for a variety of other polymeric systems, including the condensation/precipitation and subsequent redissolution of globular proteins,[48,49] DNA,[50–52] and other strong polyelectrolytes[53–55] upon varying the concentration of multivalent ions in the solution. Strong polyelectrolyte gels also display reentrant swelling in response to changes in the concentration of monovalent[56] and multivalent[57,58] salts. Acrylamide-derivative polymer gels deswell and then swell in an aqueous solution as the concentration of an organic solute is monotonically increased.[59]

Understanding the response of the material to different stimuli, in terms of its molecular structure and local chemical composition, can greatly help the optimal design of applications. We have quantified the response of the material to an applied pressure and electric potential. The dependence of the isothermal compressibility and the capacitance of the film on the composition of the solution were reported. Moreover, we have presented profiles of local pH inside and close to the solution-side surface of the hydrogel membrane. This information cannot be ignored when designing applications that pursue or require the absorption of biomolecules or pH-sensitive molecules in the interior of the film. Indeed, we are currently considering the response of the material to changes in the concentration of pH-responsive biomolecules in the buffer solution.

[1] T. Tanaka, Phys. Rev. Lett. **40**, 820 (1978).
[2] G. Chen and A. S. Hoffman, Nature (London) **373**, 49 (1995).
[3] R. Yoshida, K. Uchida, Y. Kaneko, K. Sakai, A. Kikuchi, Y. Sakurai, and T. Okano, Nature (London) **374**, 240 (1995).
[4] T. Tanaka, D. Fillmore, S.-T. Sun, I. Nishio, G. Swislow, and A. Shah, Phys. Rev. Lett. **45**, 1636 (1980).
[5] B. Zhao and J. S. Moore, Langmuir **17**, 4758 (2001).
[6] S. De, N. Aluru, B. Johnson, W. Crone, D. Beebe, and J. Moore, J. Microelectromech. Syst. **11**, 544 (2002).
[7] I. Ohmine and T. Tanaka, J. Chem. Phys. **77**, 5725 (1982).
[8] T. Tanaka, I. Nishio, S.-T. Sun, and S. Ueno-Nishio, Science **218**, 467 (1982).
[9] Y. Osada, H. Okuzaki, and H. Hori, Nature (London) **355**, 242 (1992).
[10] A. Suzuki and T. Tanaka, Nature (London) **346**, 345 (1990).
[11] M. Ilavsky, Macromolecules **15**, 782 (1982).
[12] Y. Hirokawa and T. Tanaka, J. Chem. Phys. **81**, 6379 (1984).
[13] C. M. Hassan, F. J. Doyle, and N. A. Peppas, Macromolecules **30**, 6166 (1997).
[14] T. Miyata, T. Uragami, and K. Nakamae, "Recent developments in hydrogels," Adv. Drug Deliv. Rev. **54**, 79 (2002).
[15] T. Miyata, M. Jige, T. Nakaminami, and T. Uragami, Proc. Natl. Acad. Sci. U.S.A. **103**, 1190 (2006).
[16] R. V. Ulijn, J. Mater. Chem. **16**, 2217 (2006).
[17] Y. Qiu and K. Park, Adv. Drug Deliv. Rev. **53**, 321 (2001).
[18] X. Zhang, Y. Guan, and Y. Zhang, Biomacromolecules **13**, 92 (2012).
[19] A. Sidorenko, T. Krupenkin, A. Taylor, P. Fratzl, and J. Aizenberg, Science **315**, 487 (2007).

[20] D. J. Beebe, J. S. Moore, J. M. Bauer, Q. Yu, R. H. Liu, C. Devadoss, and B.-H. Jo, Nature (London) **404**, 588 (2000).

[21] T. Tanaka and D. J. Fillmore, J. Chem. Phys. **70**, 1214 (1979).

[22] I. Tokarev and S. Minko, Soft Matter **5**, 511 (2009).

[23] M. A. C. Stuart, W. T. S. Huck, J. Genzer, M. Muller, C. Ober, M. Stamm, G. B. Sukhorukov, I. Szleifer, V. V. Tsukruk, M. Urban, F. Winnik, S. Zauscher, I. Luzinov, and S. Minko, Nat. Mater. **9**, 101 (2010).

[24] Y. Kang, J. J. Walish, T. Gorishnyy, and E. L. Thomas, Nat. Mater. **6**, 957 (2007).

[25] M. Guvendiren, D. A. Brass, P. B. Messersmith, and K. R. Shull, J. Adhesion **85**, 631 (2009).

[26] J. T. Suri, D. B. Cordes, F. E. Cappuccio, R. A. Wessling, and B. Singaram, Angew. Chem., Int. Ed. **42**, 5857 (2003).

[27] P. Kim, L. D. Zarzar, X. Zhao, A. Sidorenko, and J. Aizenberg, Soft Matter **6**, 750 (2010).

[28] M. Guvendiren, J. A. Burdick, and S. Yang, Soft Matter **6**, 2044 (2010).

[29] G. S. Longo, M. Olvera de la Cruz, and I. Szleifer, Macromolecules **44**, 147 (2011).

[30] G. S. Longo, M. Olvera de la Cruz, and I. Szleifer, Soft Matter **8**, 1344 (2012).

[31] P. Gong, J. Genzer, and I. Szleifer, Phys. Rev. Lett. **98**, 018302 (2007).

[32] Y. V. Lyatskaya, F. A. M. Leermakers, G. J. Fleer, E. B. Zhulina, and T. M. Birshtein, Macromolecules **28**, 3562 (1995).

[33] R. Israels, F. A. M. Leermakers, and G. J. Fleer, Macromolecules **27**, 3087 (1994).

[34] P. Gong, T. Wu, J. Genzer, and I. Szleifer, Macromolecules **40**, 8765 (2007).

[35] T. Wu, P. Gong, I. Szleifer, P. Vlček, V. Šubr, and J. Genzer, Macromolecules **40**, 8756 (2007).

[36] R. Nap, P. Gong, and I. Szleifer, J. Polym. Sci. Part B/Polym. Phys. **44**, 2638 (2006).

[37] See supplementary material at http://dx.doi.org/10.1063/1.4896562 for a complete description of the theory and its numerical implementation, the molecular model of the grafted film, derivation of experimental observables, and additional results.

[38] *CRC Handbook of Chemistry and Physics*, 90th ed., edited by D. R. Lide (CRC Press, Boca Raton, FL, 2010).

[39] E. B. Zhulina, T. M. Birshtein, and O. V. Borisov, Macromolecules **28**, 1491 (1995).

[40] J. K. Wolterink, J. van Male, M. A. C. Stuart, L. K. Koopal, E. B. Zhulina, and O. V. Borisov, Macromolecules **35**, 9176 (2002).

[41] A. A. Polotsky, F. A. Plamper, and O. V. Borisov, Macromolecules **46**, 8702 (2013).

[42] S. Nohara, H. Wada, N. Furukawa, H. Inoue, M. Morita, and C. Iwakura, Electrochim. Acta **48**, 749 (2003).

[43] L. Pan, G. Yu, D. Zhai, H. R. Lee, W. Zhao, N. Liu, H. Wang, B. C.-K. Tee, Y. Shi, Y. Cui, and Z. Bao, Proc. Natl. Acad. Sci. U.S.A. **109**, 9287 (2012).

[44] C. P. Smith and H. S. White, Anal. Chem. **64**, 2398 (1992).

[45] C. P. Smith and H. S. White, Langmuir **9**, 1 (1993).

[46] M. Tagliazucchi, E. J. Calvo, and I. Szleifer, J. Phys. Chem. C **112**, 458 (2008).

[47] M. Tagliazucchi, E. J. Calvo, and I. Szleifer, Langmuir **24**, 2869 (2008).

[48] F. Zhang, M. W. A. Skoda, R. M. J. Jacobs, S. Zorn, R. A. Martin, C. M. Martin, G. F. Clark, S. Weggler, A. Hildebrandt, O. Kohlbacher, and F. Schreiber, Phys. Rev. Lett. **101**, 148101 (2008).

[49] F. Zhang, S. Weggler, M. J. Ziller, L. Ianeselli, B. S. Heck, A. Hildebrandt, O. Kohlbacher, M. W. A. Skoda, R. M. J. Jacobs, and F. Schreiber, Prot.: Struct., Funct. Bioinf. **78**, 3450 (2010).

[50] E. Raspaud, M. Olvera de la Cruz, J.-L. Sikorav, and F. Livolant, Biophys. J. **74**, 381 (1998).

[51] M. Saminathan, T. Antony, A. Shirahata, L. H. Sigal, T. Thomas, and T. J. Thomas, Biochemistry **38**, 3821 (1999).

[52] T. T. Nguyen, I. Rouzina, and B. I. Shklovskii, J. Chem. Phys. **112**, 2562 (2000).

[53] M. Olvera de la Cruz, L. Belloni, M. Delsanti, J. P. Dalbiez, O. Spalla, and M. Drifford, J. Chem. Phys. **103**, 5781 (1995).

[54] F. J. Solis and M. O. de la Cruz, J. Chem. Phys. **112**, 2030 (2000).

[55] F. J. Solis and M. Olvera de laCruz, Eur. Phys. J. E **4**, 143 (2001).

[56] P. K. Jha, J. W. Zwanikken, and M. Olvera de la Cruz, Soft Matter **8**, 9519 (2012).

[57] S. G. Starodoubtsev, A. A. Lyubimov, and A. R. Khokhlov, J. Phys. Chem. B **107**, 12206 (2003).

[58] C. E. Sing, J. W. Zwanikken, and M. Olvera de la Cruz, Macromolecules **46**, 5053 (2013).

[59] S. Katayama, Y. Hirokawa, and T. Tanaka, Macromolecules **17**, 2641 (1984).